

Characterization of zincblende CuInS₂ nanostructured film: The XRD, Raman, FT-IR and UV-vis spectroscopical investigations

T Hurma*

Department of Physics, Anadolu University, TR 26470, Eskişehir, Turkey

Received 27 January 2016; revised 28 September 2016; accepted 22 November 2016

Zincblende semiconductor CuInS₂ has not been focus of studies until recently. Ultrasonic spray pyrolysis (USP) method is used to deposit zincblende CuInS₂ nanostructured film on glass substrate at 250 °C in this study. The film was characterized by vibrational (FT-IR and Raman) spectroscopy, X-ray diffraction (XRD), scanning electron microscopy (SEM) and UV-vis spectra. The crystallite size was calculated to be around 30 nm by using the well-known Scherrer equation with the peak corresponding to (111) plane. The Raman peak at 306 cm⁻¹ is assigned to the A₁ mode of the CuAu-ordered CuInS₂. Thus, metastable cubic zincblende structure would be evidenced. The absorption coefficient of the film has been found to be in the order of 10⁴-10⁵ cm⁻¹, which make it promising for an intensive optoelectronic application.

Keywords: Zincblende CuInS₂ film, XRD, Optical properties

1 Introduction

Solar energy has the potential to meet the demand if the cost of solar cell fabrication can be kept down without sacrificing efficiency. Inorganic thin film based photovoltaics may be able to overcome the high cost of its silicon counterparts while maintaining a comparable efficiency¹. The ternary compound semiconductor materials have been successfully applied as absorber layers of thin film solar cells². There are different ternary compound semiconductor materials³⁻⁵, such as CuInS₂, Cu (In,Ga)Se₂, and CuInSe₂. Among semiconductor materials, CuInS₂ is one of the most promising alternative absorber materials for the development of thin film solar cells⁶⁻¹¹. The stoichiometric ratio, crystal structure, morphology and photovoltaic property of CuInS₂ are influenced strongly by the preparation method¹². At room temperature, stable phases in the Cu-In-S system, two ternary compounds could be formed CuInS₂ and CuIn₅S₈. CuInS₂ exists in three modifications (i) CuInS₂-chalcopyrite (CH) structure, (ii) CuInS₂-zincblende CuAu (CA) and (iii) CuInS₂-wurtzite CuPt (CP) two metastable structures depending on the temperature, CuIn₅S₈ has a cubic spinel structure over the whole temperature range from 20 °C up to the melting point at 1085°C^{13,14}. A conventional XRD study is usually incapable to assign the chalcopyrite CH and the zincblende CA

phase of CuInS₂ due to the overlapping of almost all XRD peaks¹⁵. By means of Raman spectroscopy, the different crystalline phases of CuInS₂, such as the CH and the CA phase, can be distinguished¹⁶. Raman is a complimentary spectroscopic technique for identification of unknown materials, structural quality and the secondary phases in the films. The combination of both methods yields a detailed insight into the growth path of CuInS₂, as by XRD the entire absorber volume can be investigated, whereas Raman spectroscopy is sensitive to the surface-near region (information depth of around 150 nm). More frequently used methods for the preparation of CuInS₂ include a chemical bath deposition¹⁷, thermal evaporation¹⁸, aerosol-assisted chemical vapor deposition¹⁹, modulated flux evaporation²⁰, molecular beam epitaxy²¹, electrodeposition²², and ultrasonic spray pyrolysis²³⁻²⁵, etc. Earlier and may be more recent experimental studies have been mostly devoted to tetragonal chalcopyrite CuInS₂ films. In this study, cubic zincblende nanostructured CuInS₂ film has been deposited. Raman and FT-IR spectra of the film have been necessary to deepen in the physicochemical properties of the material. Therefore, other experimental techniques, such as X-ray diffraction, scanning electron microscopy and UV-vis spectra have been used in order to achieve accurate knowledge of the crystalline properties of the zincblende CuInS₂ film.

*E-mail: tulayhurma@gmail.com

2 Experimental Details

CuInS₂ film can be deposited using a variety of metal salts and sulfur sources. In this study CuInS₂ film has been produced by spraying the aqueous solution 40 mL of CuCl₂·2H₂O (98 % Aldrich), 10 mL of InCl₃ (98% Aldrich) and 25 mL of SC(NH₂)₂ (98% Aldrich) as Cu, In and S sources, respectively. Totally 75 mL of solution was sprayed onto glass substrates that were previously heated for 15 min. Substrate temperature was kept constant at 250 °C. The experimental setup and the other experimental details are explained elsewhere²⁶. The chemical solution was atomized into the stream of the fine droplets via ultrasonic spray-head, which contains 58 kHz transducer. The ultrasonic spray-head to substrate distance was approximately 30 cm. The flow rate of solution which was controlled with a flow meter and carrier gas pressure during spraying was adjusted to be 5 mL/min and 0.2 kg/cm², respectively. Nitrogen was used as the carrier gas. After deposition, the film was allowed to cool down to room temperature and then taken out for further characterization. The deposited film was uniform, smooth and well adherent to the substrate. The obtained film was characterized by XRD using a RIGAKU D/max 220H X-ray diffractometer with graphite monochromatized CuK_α radiation ($\lambda=1.5405 \text{ \AA}$). The XRD pattern was scanned in 2θ range of 20°–60°. The surface morphology of the film was characterized by scanning electron microscopy (SEM; JEOL JSM-5600LV) and atomic force microscopy (AFM; Solver PRO-NSG20). The Raman spectrum of the film was recorded in 200–700 cm⁻¹ range on a Bruker Senterra Dispersive Raman instrument using laser excitation with the wavelength of 632.8 nm. The Fourier transform infrared (FT-IR) spectrum was recorded on Perkin Elmer 2000 FT-IR spectrometer in the range of 500–3000 cm⁻¹ using ATR (4 cm⁻¹ resolution). The optical measurements of CuInS₂ film were carried out in room temperature using Perkin Elmer Lambda 2S UV/VIS spectrophotometer in the wavelength range from 300 to 1050 nm.

3 Results and Discussion

3.1 X-ray diffraction analysis

The crystalline structure and orientation of the deposited film was investigated by XRD. The XRD pattern of CuInS₂ film deposited onto the glass substrate is shown in Fig. 1. The presence of sharp structural peak in this X-ray diffraction pattern confirmed the polycrystalline nature of the film. The

film exhibits four clear peaks related to (200), (220), (311) plane at 32.49°, 46.56°, 55.20° and shows strong preferential orientation of (111) plane at $2\theta=28.10^\circ$. All the diffraction peaks have a good match to the previous reported zinc blende-structure²⁷ CuInS₂, which brings great interest in this structure. XRD pattern shows abroad hump-like feature in the range of 20°–40° which can be attributed to the amorphous nature of glass substrate. Crystallites are coherent diffraction domains in X-ray diffraction. XRD can be used for calculating crystalline size by using well-known Scherrers formula²⁸. An idea about the particle size is obtained from the SEM photograph and it helps to arrive on the range of particle size. The actual particle size can be larger than “XRD crystallite size” calculated from Scherrer equation. The crystallite size of the film was calculated to be around 30 nm by using the Scherrer equation with the peak corresponding to the (111) plane.

3.2 Raman and FTIR analysis

FTIR and Raman are complimentary spectroscopic techniques which provide direct information about the vibrational properties of crystalline materials. Figure 2 shows the Raman spectrum of CuInS₂ film in the frequency region 200–700 cm⁻¹. The Raman spectrum studies revealed two peaks (306 and 482 cm⁻¹) of the film. The Raman A1 mode²⁹ of the CH structure is centered at 290 cm⁻¹. For metastable CA structure³⁰, the Raman A1 mode is observed at around 305 cm⁻¹. Therefore the peak at 306 cm⁻¹ is assigned to the A1 mode of the CA-ordered CuInS₂. Thus, metastable cubic zincblende CA structure would be evidenced. The peak at 482 cm⁻¹ may be assigned to the secondary CuS^{22,31,32} phonon mode. In contrast to the Raman

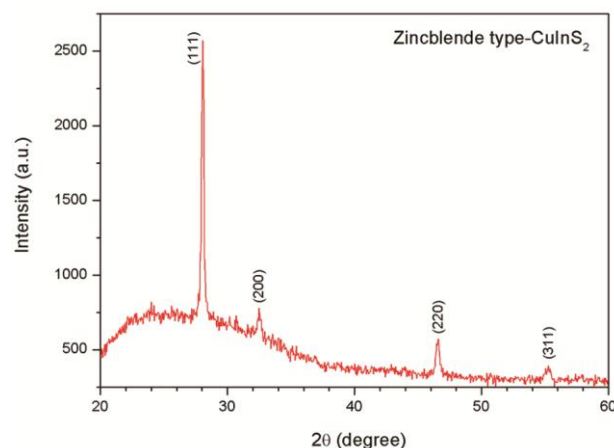


Fig. 1 – XRD pattern of zincblende CuInS₂ nanostructured film

data presented here no CuS phase has been observed with XRD. Therefore, it is likely that CuS forms near the surface with a relatively small volume percentage and can only be detected by Raman. This is related to relatively high Raman method cross section of CuS , and makes the Raman method very sensitive to the presence of this secondary phase. The shoulder around 348 cm^{-1} is probably relating to CuIn_5S_8 phase³³. XRD measurement did not detect the existence of the CuIn_5S_8 and CuS phases. It would be difficult to detect or identify via XRD any phase if it has a very small volume percentage of crystallites and has almost identical lattice parameters with another phase. Contrary to X-ray diffraction, Raman spectroscopy is especially sensitive to the local symmetry. Raman spectroscopy is an approved method to study qualitative and quantitative contribution of the CuInS_2 phases^{29,30,34} as well as possible secondary phases³⁵. Figure 3 shows the FT-IR spectrum of the deposited film within a wavelength spectrum ranging from $500\text{-}3000 \text{ cm}^{-1}$. The absorption peaks observed between 2295 and 2389 cm^{-1} is because of the existence of CO_2 molecule in air and are not related to the film. The weak band at about 800 cm^{-1} may be assigned to the ν (SCN) in sulfur- coordinated thiourea. The strong band corresponding to 1186 cm^{-1} indicates the presence of ν (C=S) symmetric stretching. Metals should not show any FT-IR absorption. Infrared absorption is based on a nonzero transition dipole moment of vibrational modes. Metals certainly have vibrational modes, but light cannot activate it.

3.3 Surface morphology

Figure 4 shows SEM image of the zincblende CuInS_2 nanostructured film at 100000 magnification. The image in Fig. 4 demonstrates that the deposited

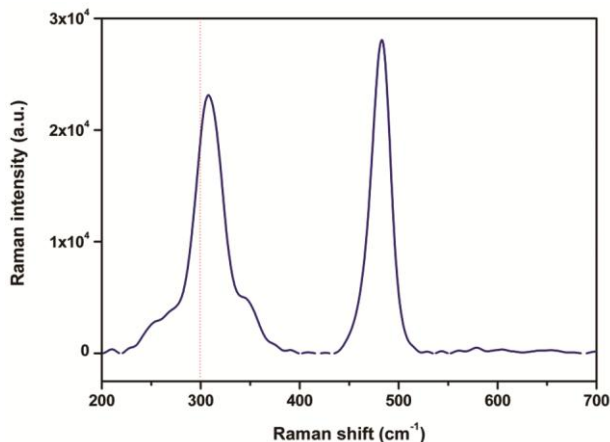


Fig. 2 – Raman spectrum of zincblende CuInS_2 nanostructured film

CuInS_2 film has a granular morphology, and good surface coverage, good crystallinity can be seen where as there are no cracks (pin hole) on the surface of the film. The nanosize of particles of the film was estimated from the SEM image that consistend with XRD analysis.

3.4 Optical properties

The optical absorption and transmittance spectra for zincblende CuInS_2 film in the wavelength range of $200\text{-}1100 \text{ nm}$ are shown in Fig. 5. There is a high absorbance in region up to 370 nm wavelength, then absorbance decreases. Transmittance first increases quite sharply and in wavelength the value reaches to a maximum and then slowly decreases, and again increases and reaches to maximum value. It can be seen that film has two step transitions. The occurrence of two slopes in the transmission edge region means that film was not single phase material, and probably surface and bulk imperfections affect the

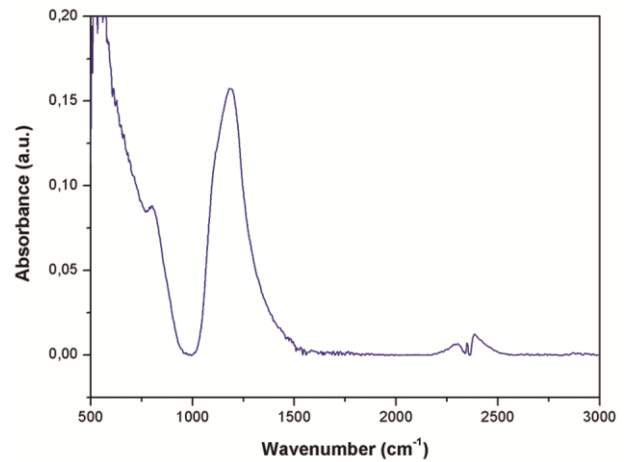


Fig. 3 – FT-IR spectrum of zincblende CuInS_2 nanostructured film

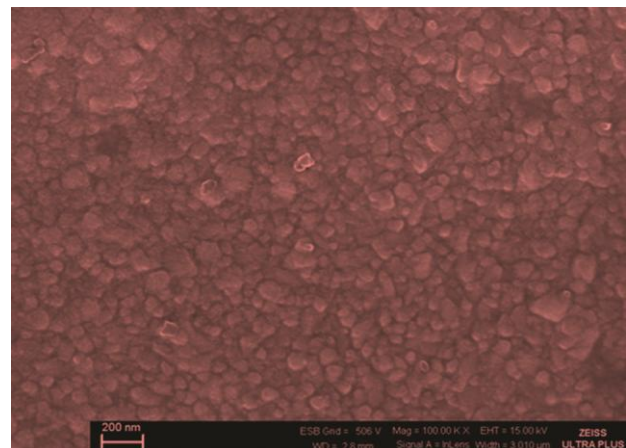


Fig. 4 – SEM image of zincblende CuInS_2 nanostructured film

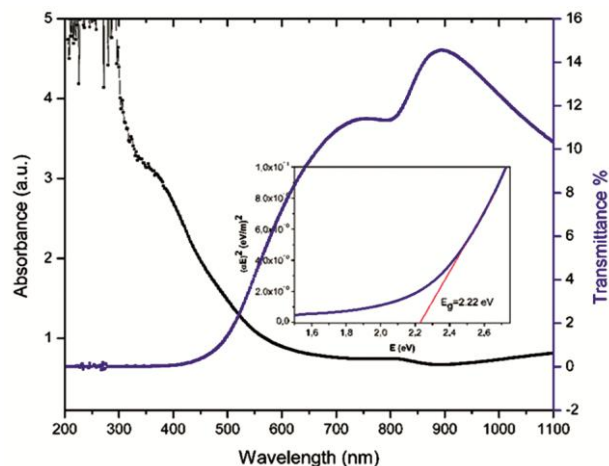


Fig. 5 – UV-vis absorption and transmittance spectrum (inset the plot of $(\alpha hv)^2$ vs $h\nu$) of zincblende CuInS_2 film

optical properties. This is in agreement with the Raman results. The absorption coefficient has been determined and is found to be in 10^4 - 10^5 cm^{-1} range, one of the highest among semiconductors³⁶. This result is very important because it is known that the spectral dependence of the absorption coefficient affects the solar conversion efficiency. Inset of Fig. 5 shows curves of $(\alpha hv)^2$ against $h\nu$ for the zincblende CuInS_2 nanostructured film. The curve has a good straight line fit over higher energy range above the absorption edge, which is indicative of a direct optical transition near the absorption edge. Based on the inset of Fig. 5, the direct energy gap E_g of the film has been calculated and it is found to be 2.22 eV. Although the band gap energy of bulk CuInS_2 is within 1.4 -1.5 eV³⁷, prepared zinc blende nanostructured CuInS_2 film was outside the range at 2.2 eV. The increase in the band gap has been may be attributed to the defects and secondary phases. But it is well known that when the size of particles decrease into the nanoscale range, the band gap will increase due to quantum confinement effects, which means that smaller size leads to a larger band gap energy^{38,39}. This film is a promising compound for development of various solid state devices including the blue light emitting diodes, laser diodes, solar cells, microwave devices and various optoelectronic devices.

4 Conclusions

In this paper, the structural properties, surface morphology, vibrational (FT-IR and Raman), and optical properties of zincblende CuInS_2 nanostructured film deposited by USP method are investigated. The XRD pattern of the film shows that CuInS_2 film

is polycrystalline in nature and strongly oriented along the (111) direction with zincblende structure. The Raman (200-700 cm^{-1}) and FT-IR (500-3000 cm^{-1}) spectra of the film were recorded. Raman spectrum revealed that the peak at 306 cm^{-1} can be assigned to the A1 mode of the zincblende CuInS_2 . The Raman analysis also shows that there exist a CuS phase on the surface of the film. In FT-IR spectrum, the two bands observed correspond to $\nu(\text{SCN})$ in sulfur- coordinated thiourea (800 cm^{-1}) and $\nu(\text{C}=\text{S})$ symmetric stretching (1186 cm^{-1}) of the film. The absorption coefficient has been determined and is found to be in the order of 10^4 - 10^5 cm^{-1} and the optical band gap of the film was found to be 2.22 eV with a direct optical transition.

Acknowledgement

We would like to thank Mrs Tülay Tıraş and Özge Bağlayan for the Raman and FT-IR spectroscopy measurements.

References

- 1 Tapley A, Hart C, Vaccarello D, Love D A & Ding Z F, *J Electrochem Soc*, 161 (2014) 725.
- 2 Hussain K M A, Podder J & Saha D K, *Indian J Pure Appl Phys*, 20 (2012) 117.
- 3 Siemer K, Klaer J, Luck I, Bruns J, Klenk R & Braunig D, *Solar Energ Mater Solar Cells*, 67 (2001) 159.
- 4 Gabor A M, Tuttle J R, Albin D S, Contreras M A, Noufi R & Hermann A M, *Appl Phys Lett*, 65 (1994) 198.
- 5 Abushama J A M, Johnston S, Moriarty T, Teeter G, Ramanathan K & Noufi R, *Prog Photovolt: Res Appl*, 12 (2004) 39.
- 6 Noufi R, Axton R, Herrington C & Deb S K, *Appl Phys Lett*, 45 (1984) 668.
- 7 Krustok J, Raudoja J & Collan H, *Thin Solid Films*, 387 (2001) 195.
- 8 Goto H, Hashimoto Y & Ito K, *Thin Solid Films*, 552 (2004) 451.
- 9 Chang W S, Wu C C, Jeng M S, Cheng K W, Huang CM & Lee T C, *Mater Chem Phys*, 120 (2010) 307.
- 10 Repins I, Contreras M A, Egaas B, De Haet C, Scharf J, Perkins C L, To B & Noufi R, *Prog Photovolt: Res Appl*, 16 (2008) 235.
- 11 Klenk R, Klaer J, Scheer R, Lux S M C, Luck I, Meyer N & Ruhle U, *Thin Solid Films*, 480 (2005) 509.
- 12 Zhang Y, He W & Jia H, *Phys Scripta*, 88 (2013) 015705.
- 13 Kazmerski L L & Wagner S, *Current topics in photovoltaics* 1, (Academic Press, New York) (1985) 279.
- 14 Riedle T, *Raman spectroscopy for the analysis of thin CuInS_2 films*, PhD Thesis, Technical University of Berlin, 2002.
- 15 Alvarez G J, *Characterization of CuInS_2 films for solar cell application by Raman spectroscopy*, PhD thesis, University of Barcelona, Barcelona, Spain, 2002.
- 16 Sheng X, Wang L, Luo Y & Yang D, *Nanoscale Res Lett*, 6 (2011)562.
- 17 Pathan H M & Lokhande C D, *Appl Surf Sci*, 239 (2004) 11.

- 18 Ben R M, Khedmi N, Fodha M A & Kanzari M, *Energy Procedia*, 44 (2014) 52.
- 19 Jin M H C, Banger K K, Harris J D & Hepp A F, *Mater Sci Eng B*, 116 (2005) 395.
- 20 Guillen C, Herrero J, Gutierrez M & Briones F, *Thin Solid Films*, 480 (2005) 19.
- 21 Alvarez G J, Barcones B, Perez R A , Romano R A , Morante J R, Janotti A, Wei S H & Scheer R, *Phys Rev B*, 71 (2005) 054303.
- 22 Yukawa T, Kuwabara K & Koumoto K, *Thin Solid Films*, 286 (1996) 151.
- 23 Bihri H, Messaoudi C, Sayah D, Boyer A, Mzerd A & Abd L M, *Phys Stat Sol*, 129 (1992) 193.
- 24 Krunks M, Bijakina O, Mikli V, Rebane H, Varema T, Altosaar M & Mellikov E, *Solar Energ Mater Solar Cells*, 69 (2001) 93.
- 25 Ortega L M & Morales A A, *Thin Solid Films*, 330 (1998) 96.
- 26 Özer T & Köse S, *Int J Hydrogen Energ*, 34 (2009) 5186.
- 27 Pan D, An L, Sun Z, Hou W, Yang Y, Yang Z & Lu Y, *J Am Chem Soc*, 130 (2008) 5620.
- 28 Antony A, Asha A S, Yoosuf Y, Manoj R & Jayaraj M K, *Sol Energ Mat Sol Cells*, 81 (2004) 407.
- 29 Alvarez G J, Marcos R J, Perez R A, Romano R A, Morante J R & Scheer R, *Thin Solid Films*, 361 (2000) 208.
- 30 Alvarez G J, Rodriguez A P, Barcones B, Rodriguez A R, Morante J R, Janotti A, Wei S H & Scheer R, *Appl Phys Lett*, 80 (2002) 562.
- 31 Rudigier E, *Phase transformations and crystalline quality of CuInS₂ thin films*, Ph.D. Thesis 2004, Philipps University of Marburg.
- 32 Minceva-Sukarova B, Najdoski M, Grozdanov I & Chunnillall C J, *J Mol Struct*, 410 (1997) 267.
- 33 Oja I, Nanu M, Katerski A, Krunks M, Mere A, Raudoja J & Goossens A, *Thin Solid Films*, 480 (2005) 82.
- 34 Hurma T & Kose S, *Optik*, 127 (2016) 3779
- 35 Guha P, Das D, Maity A B, Ganguli D & Chaudhuri S, *Sol Energ Mat Sol Cells*, 80 (2003) 115.
- 36 Yakushev M V, Martin R W, Mudryi A V & Ivaniukovich A V, *Appl Phys Lett*, 92 (2008) 111908.
- 37 Yakushev M V, Mudryi A V, Victorov I V, Krustok J & Mellikov E, *Appl Phys Lett*, 88 (2006) 011922.
- 38 Steigerwald M L & Brus L E, *Accounts Chem Res*, 23 (1990) 183.
- 39 Alivisatos A P, *J Phys Chem*, 100 (1996) 13226.